Magnetic properties of organolanthanide(II) complexes, from electronic structure and crystal field effect

Eduardo Solís-Cespedes[1,2], Dayán Páez-Hernández[3,4*]

June 4, 2021

[1]Escuela de Bioingeniería Médica, Facultad de Medicina, Universidad Católica del Maule.

[2]Laboratorio de Bioinformática y Química Computacional, Facultad de Medicina, Universidad Católica del Maule

[3]Center of Applied Nanoscience (CANS), Universidad Andres Bello, República 330, Santiago, Chile.

[4]Departamento de Ciencias Químicas, Universidad Andres Bello, República 275, Santiago, Chile.

Supporting Information

Electronic structure

Table 1: One-electron Condon-Slater F^k $(k = 2, 4, 6)$ and effective spin-orbit coupling parameters obtained from ab-initio ligand field approximation (AILF) for Eu^{2+} free ion and complexes

Molecule	$\mathbf{F}^2$	$\mathbf{F}^4$	$\mathbf{F}^6$	ξ
Eu^{2+}	106475	66500	47756	1273
$Eu(CNT)_2$ (D_{9h})	104356 (2%)	65249 (2%)	46838 (1.9%)	1142
$Eu(CNT)_2$ (D_{9d})	104257 (2%)	65198 (1.9%)	46798 (2%)	1141
$EuCp_3^-$ (C_{3v})	105119 (0.8%)	65657 (1.3%)	47146 (1.3%)	1264

Table 2: One-electron Condon-Slater F^k $(k = 2, 4, 6)$ and effective spin-orbit coupling parameters obtained from ab-initio ligand field density functional theory approximation (LFDFT) for Eu^{2+} free ion and complexes

Molecule	$\mathbf{F}^2$	$\mathbf{F}^4$	$\mathbf{F}^6$	ξ
Eu^{2+}	99062	61472	44032	1293
$Eu(CNT)_2$ (D_{9h})	84459 (14.7%)	52430 (14.7%)	37562 (14.7%)	1204
$Eu(CNT)_2$ (D_{9d})	84470 (14.7%)	52438 (14.7%)	37567 (14.7%)	1204
$EuCp_3^-$ (C_{3v})	81945 (17.3%)	50885 (17.3%)	36458 (17.3%)	1189

Table 3: Electronic configuration of the SF-states corresponding to the splitting of the ^8S manifold in $[Cp_3Eu]^-$ and $[Eu(COT)_2]^{2-}$ model complex

	$[EuCp_3]^-$ (C_{3v})	
State	Config	%
$^8A_1$	$a_1^2a_2^2f_0^1f_{-1}^1f_{+1}^1f_{-2}^1f_{+2}^1f_{-3}^1f_{+3}^1d_0^0$	100%
$^8A_1$	$a_1^2a_2^2f_0^1f_{-1}^1f_{+1}^1f_{-2}^1f_{+2}^1f_{-3}^0f_{+3}^1d_0^1$	100%
$^8A_2$	$a_1^2a_2^2f_0^1f_{-1}^1f_{+1}^1f_{-2}^1f_{+2}^1f_{-3}^1f_{+3}^0d_0^1$	100%
^8E	$a_1^2a_2^2f_0^1f_{-1}^1f_{+1}^1f_{-2}^1f_{+2}^0f_{-3}^1f_{+3}^1d_0^1$	87%
	$a_1^2a_2^2f_0^1f_{-1}^1f_{+1}^0f_{-2}^1f_{+2}^1f_{-3}^1f_{+3}^1d_0^1$	13%
	$a_1^2a_2^2f_0^1f_{-1}^1f_{+1}^1f_{-2}^0f_{+2}^1f_{-3}^1f_{+3}^1d_0^1$	87%
	$a_1^2a_2^2f_0^1f_{-1}^0f_{+1}^1f_{-2}^1f_{+2}^1f_{-3}^1f_{+3}^1d_0^1$	13%
^8E	$a_1^2a_2^2f_0^1f_{-1}^1f_{+1}^0f_{-2}^1f_{+2}^1f_{-3}^1f_{+3}^1d_0^1$	42%
	$a_1^2a_2^2f_0^1f_{-1}^0f_{+1}^1f_{-2}^1f_{+2}^1f_{-3}^1f_{+3}^1d_0^1$	46%
	$a_1^2a_2^2f_0^1f_{-1}^1f_{+1}^1f_{-2}^1f_{+2}^0f_{-3}^1f_{+3}^1d_0^1$	6%
	$a_1^2a_2^2f_0^1f_{-1}^1f_{+1}^1f_{-2}^0f_{+2}^1f_{-3}^1f_{+3}^1d_0^1$	6%
	$a_1^2a_2^2f_0^1f_{-1}^1f_{+1}^0f_{-2}^1f_{+2}^1f_{-3}^1f_{+3}^1d_0^1$	46%
	$a_1^2a_2^2f_0^1f_{-1}^0f_{+1}^1f_{-2}^1f_{+2}^1f_{-3}^1f_{+3}^1d_0^1$	42%
	$a_1^2a_2^2f_0^1f_{-1}^1f_{+1}^1f_{-2}^1f_{+2}^0f_{-3}^1f_{+3}^1d_0^1$	6%
	$a_1^2a_2^2f_0^1f_{-1}^1f_{+1}^1f_{-2}^0f_{+2}^1f_{-3}^1f_{+3}^1d_0^1$	6%
$^8A_1$	$a_1^2a_2^2f_0^0f_{-1}^1f_{+1}^1f_{-2}^1f_{+2}^1f_{-3}^1f_{+3}^1d_0^1$	100%

Table 4: Electronic configuration of the SF-states corresponding to the splitting of the ^8S manifold in $Eu(CNT)_2$ model complex considering two groups of symmetry

	$Eu(CNT)_2$ (D_{9d})			$Eu(CNT)_2$ (D_{9h})	
State	Config	%	State	Config	%
$^8A_{2u}$	$e^2_{2u}e^2_{2u}f^1_0f^1_{-1}f^1_{+1}f^1_{-2}f^1_{+2}f^1_{-3}f^1_{+3}d^0_0$	100%	$^8A_2^{''}$	$e_2^{''2}e_2^{''2}f^1_0f^1_{-1}f^1_{+1}f^1_{-2}f^1_{+2}f^1_{-3}f^1_{+3}d^0_0$	100%
$^8E_{2g}$	$e^2_{2u}e^2_{2u}f^1_0f^1_{-1}f^1_{+1}f^0_{-2}f^1_{+2}f^1_{-3}f^1_{+3}d^1_0$	76%	$^8E_2^{'}$	$e_2^{''2}e_2^{''2}f^1_0f^1_{-1}f^1_{+1}f^1_{-2}f^0_{+2}f^1_{-3}f^1_{+3}d^1_0$	78%
	$e^2_{2u}e^1_{2u}f^1_0f^1_{-1}f^1_{+1}f^1_{-2}f^1_{+2}f^1_{-3}f^1_{+3}d^1_0$	24%		$e_2^{''2}e_2^{''1}f^1_0f^1_{-1}f^1_{+1}f^1_{-2}f^1_{+2}f^1_{-3}f^1_{+3}d^1_0$	22%
	$e^2_{2u}e^2_{2u}f^1_0f^1_{-1}f^1_{+1}f^1_{-2}f^0_{+2}f^1_{-3}f^1_{+3}d^1_0$	76%		$e_2^{''2}e_2^{''2}f^1_0f^1_{-1}f^1_{+1}f^0_{-2}f^1_{+2}f^1_{-3}f^1_{+3}d^1_0$	78%
	$e^1_{2u}e^2_{2u}f^1_0f^1_{-1}f^1_{+1}f^1_{-2}f^1_{+2}f^1_{-3}f^1_{+3}d^1_0$	24%		$e_2^{''1}e_2^{''2}f^1_0f^1_{-1}f^1_{+1}f^1_{-2}f^1_{+2}f^1_{-3}f^1_{+3}d^1_0$	22%
$^8E_{1g}$	$e^2_{2u}e^2_{2u}f^1_0f^0_{-1}f^1_{+1}f^1_{-2}f^1_{+2}f^1_{-3}f^1_{+3}d^1_0$	100%	$^8E_1^{''}$	$e_2^{''2}e_2^{''2}f^1_0f^1_{-1}f^0_{+1}f^1_{-2}f^1_{+2}f^1_{-3}f^1_{+3}d^1_0$	100%
	$e^2_{2u}e^2_{2u}f^1_0f^1_{-1}f^0_{+1}f^1_{-2}f^1_{+2}f^1_{-3}f^1_{+3}d^1_0$	100%		$e_2^{''2}e_2^{''2}f^1_0f^0_{-1}f^1_{+1}f^1_{-2}f^1_{+2}f^1_{-3}f^1_{+3}d^1_0$	100%
$^8E_{3g}$	$e^2_{2u}e^2_{2u}f^1_0f^1_{-1}f^1_{+1}f^1_{-2}f^1_{+2}f^1_{-3}f^0_{+3}d^1_0$	100%	$^8E_3^{''}$	$e_2^{''2}e_2^{''2}f^1_0f^1_{-1}f^1_{+1}f^1_{-2}f^1_{+2}f^1_{-3}f^0_{+3}d^1_0$	100%
	$e^2_{2u}e^2_{2u}f^1_0f^1_{-1}f^1_{+1}f^1_{-2}f^1_{+2}f^0_{-3}f^1_{+3}d^1_0$	100%		$e_2^{''2}e_2^{''2}f^1_0f^1_{-1}f^1_{+1}f^1_{-2}f^1_{+2}f^0_{-3}f^1_{+3}d^1_0$	100%
$^8A_{1g}$	$e^2_{2u}e^2_{2u}f^0_0f^1_{-1}f^1_{+1}f^1_{-2}f^1_{+2}f^1_{-3}f^1_{+3}d^1_0$	100%	$^8A_1^{'}$	$e_2^{''2}e_2^{''2}f^0_0f^1_{-1}f^1_{+1}f^1_{-2}f^1_{+2}f^1_{-3}f^1_{+3}d^1_0$	100%

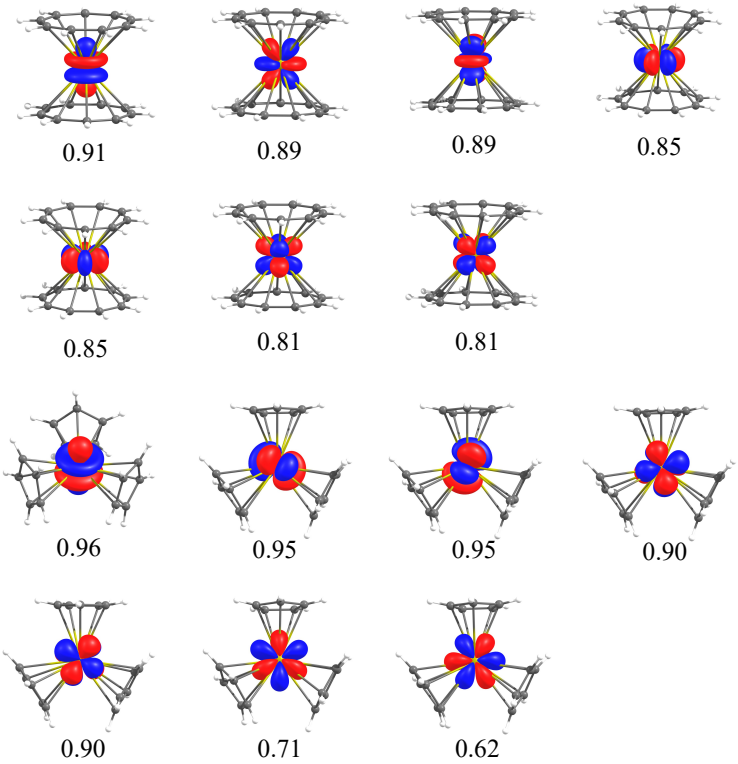

Figure 1: Selected natural orbitals and occupation numbers obtained for Sm (II) complexes from spin-orbit calculations

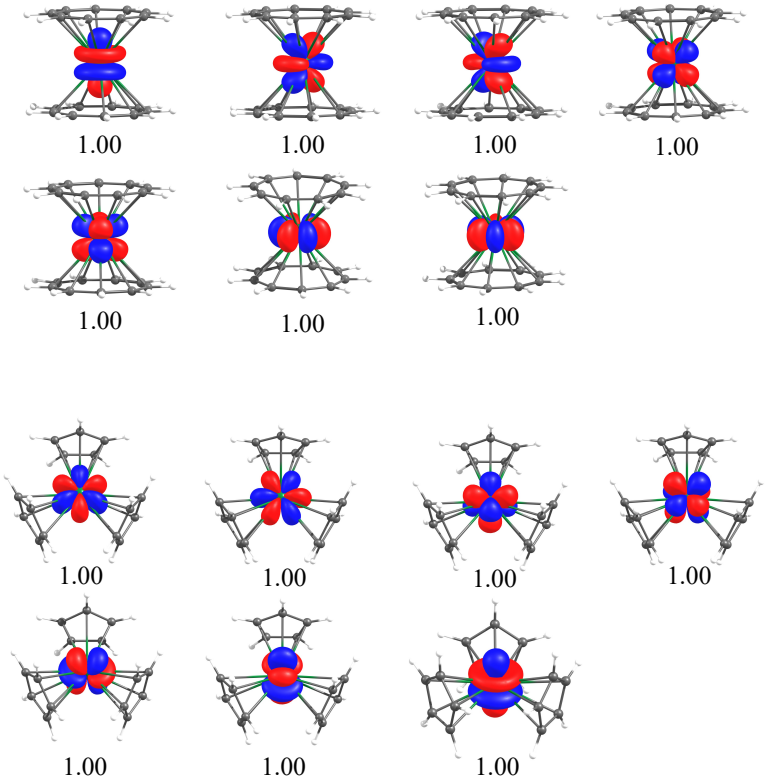

Figure 2: Selected natural orbitals and occupation numbers obtained for Eu (II) complexes from spin-orbit calculations

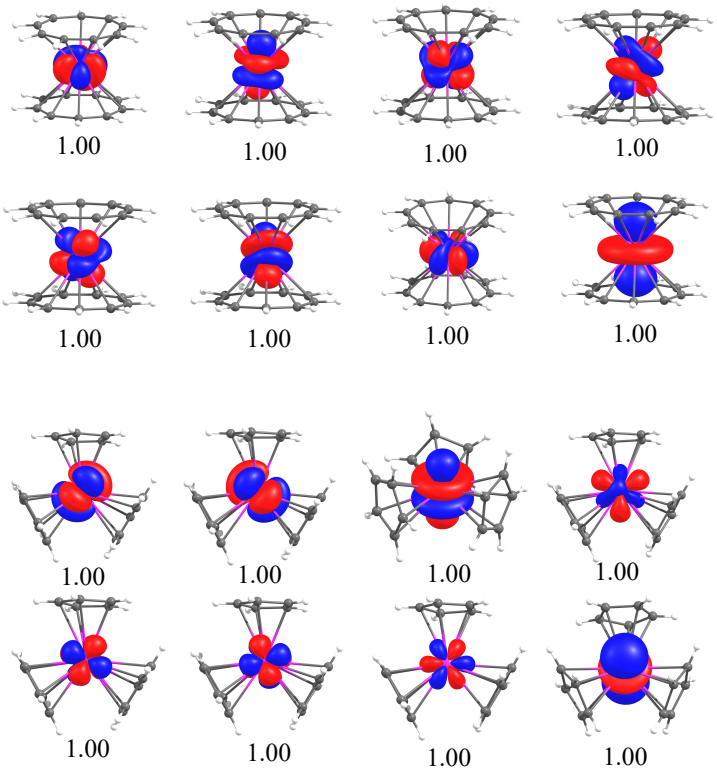

Figure 3: Selected natural orbitals and occupation numbers obtained for Gd (II) complexes from spin-orbit calculations

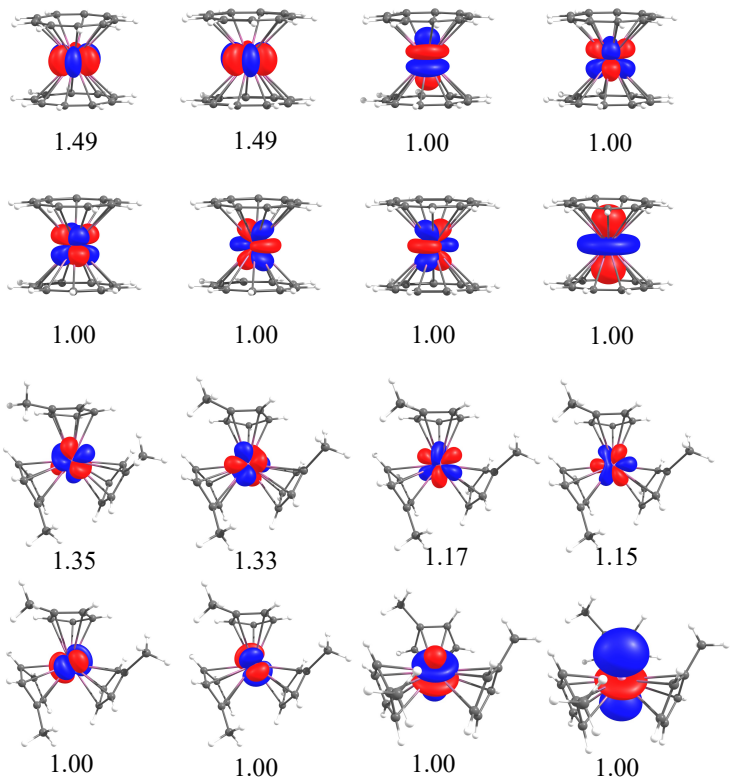

Figure 4: Selected natural orbitals and occupation numbers obtained for Tb (II) complexes from spin-orbit calculations

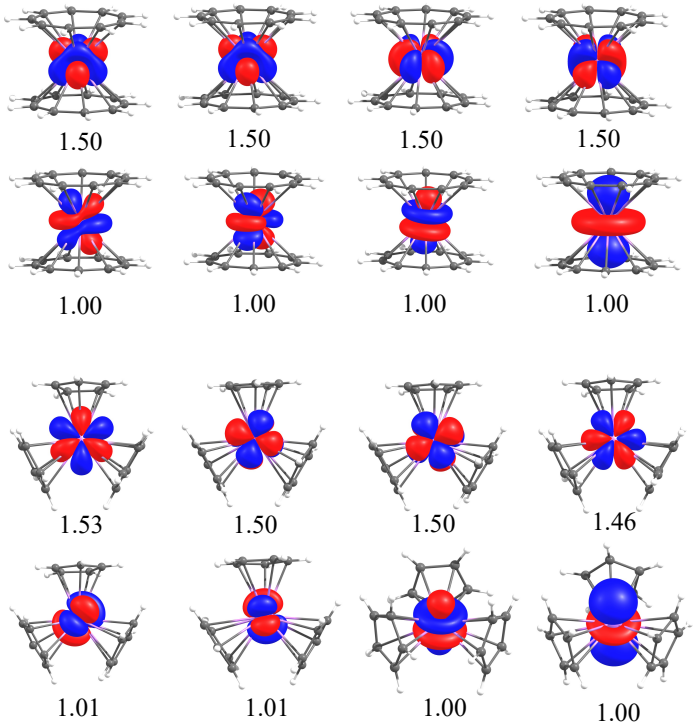

Figure 5: Selected natural orbitals and occupation numbers obtained for Dy (II) complexes from spin-orbit calculations

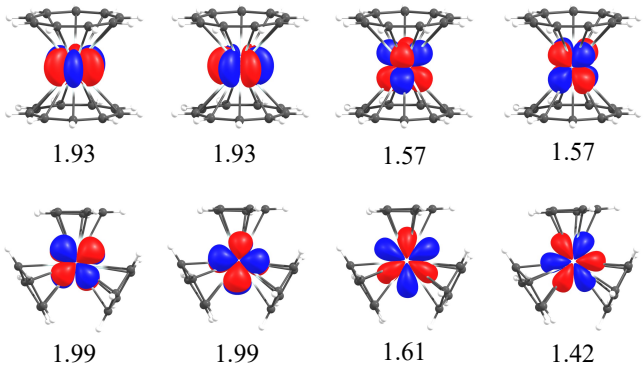

Figure 6: Selected natural orbitals and occupation numbers obtained for Tm (II) complexes from spin-orbit calculations

Magnetic properties

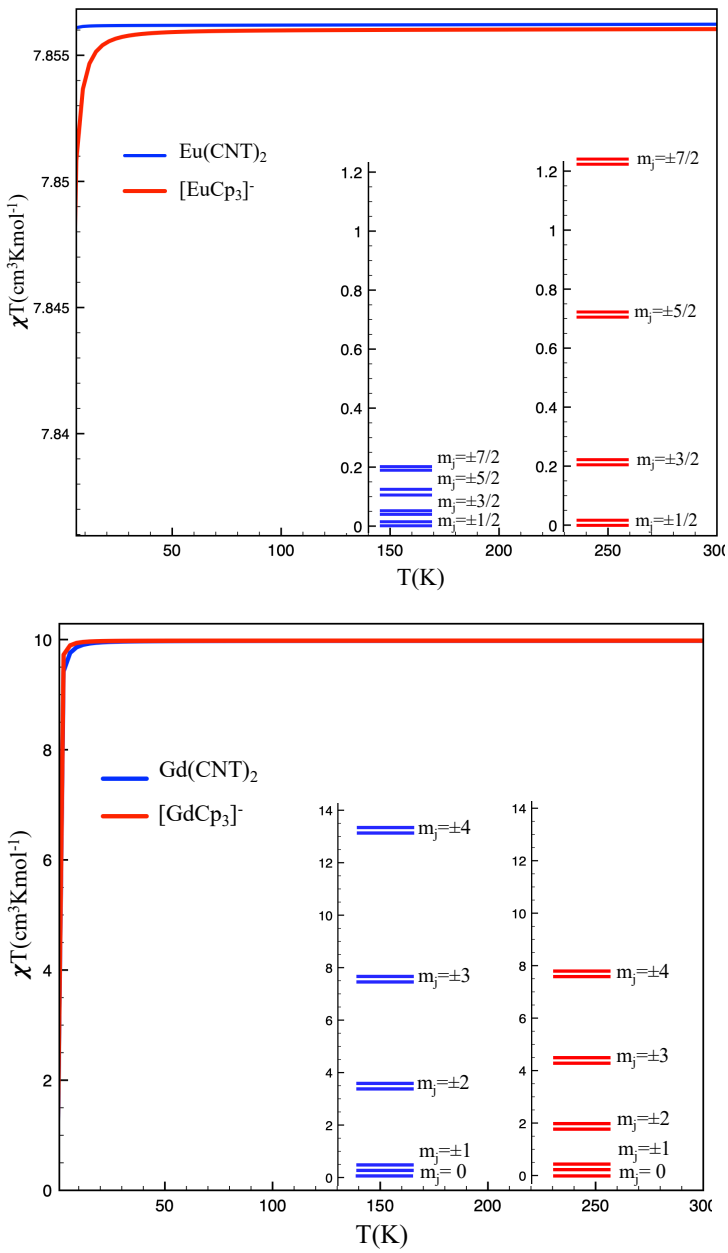

Figure 7: Calculated molar magnetic susceptibility χT $\left(cm^3 K mol^{-1}\right)$ of Eu^{2+} and Gd^{2+} complexes. The energy diagrams for the low-lying states appears insert

Table 5: Composition of the lowest Kramers doublets of Eu^{2+} complexes and their g-factors

State	**Config**	$\mathbf{g}_x$	$\mathbf{g}_y$	$\mathbf{g}_z$
	Eu(CNT)$_2$			
KD1	$85\% \mid \frac{7}{2};+\frac{1}{2}>+ 15\% \mid \frac{7}{2};-\frac{1}{2}>$	8.344	7.629	1.993
	$85\% \mid \frac{7}{2};-\frac{1}{2}>+ 15\% \mid \frac{7}{2};+\frac{1}{2}>$			
KD2	$53\% \mid \frac{7}{2};+\frac{3}{2}> + 47\% \mid \frac{7}{2};-\frac{3}{2}>$	0.338	0.377	5.987
	$53\% \mid \frac{7}{2};-\frac{3}{2}> + 47\% \mid \frac{7}{2};+\frac{3}{2}>$			
KD3	$95\% \mid \frac{7}{2};+\frac{5}{2}> + 5\% \mid \frac{7}{2};-\frac{5}{2}>$	0.004	0.029	9.986
	$95\% \mid \frac{7}{2};-\frac{5}{2}> + 5\% \mid \frac{7}{2};+\frac{5}{2}>$			
KD4	$100\% \mid \frac{7}{2};+\frac{7}{2}>$	0.013	0.013	13.980
	$100\% \mid \frac{7}{2};-\frac{7}{2}>$			
	[EuCp$_3$]$^-$			
KD1	$60\% \mid \frac{7}{2};-\frac{1}{2}> + 40\% \mid \frac{7}{2};+\frac{1}{2}>$	8.623	7.338	1.984
	$60\% \mid \frac{7}{2};+\frac{1}{2}> + 40\% \mid \frac{7}{2};-\frac{1}{2}>$			
KD2	$63\% \mid \frac{7}{2};-\frac{3}{2}> + 37\% \mid \frac{7}{2};+\frac{3}{2}>$	0.634	0.650	5.978
	$63\% \mid \frac{7}{2};+> + 37\% \mid \frac{7}{2};-\frac{3}{2}>$			
KD3	$80\% \mid \frac{7}{2};-\frac{5}{2}> + 320\% \mid \frac{7}{2};+\frac{5}{2}>$	0.009	0.010	9.985
	$80\% \mid \frac{7}{2};+\frac{5}{2}> + 320\% \mid \frac{7}{2};-\frac{5}{2}>$			
KD4	$100\% \mid \frac{7}{2};+\frac{7}{2}>$	0.000	0.000	13.980
	$100\% \mid \frac{7}{2};-\frac{7}{2}>$			

Table 6: Composition of the lowest Kramers doublets of Tm^{2+} complexes and their g-factors

State	Config	g_x	g_y	g_z
	Tm(CNT)$_2$			
KD1	$100\% \mid \frac{7}{2};+\frac{5}{2}>$	0.007	0.007	5.722
	$100\% \mid \frac{7}{2};-\frac{5}{2}>$			
KD2	$100\% \mid \frac{7}{2};+\frac{7}{2}>$	0.007	0.007	7.998
	$100\% \mid \frac{7}{2};-\frac{7}{2}>$			
KD3	$98\% \mid \frac{7}{2};+\frac{3}{2}> + 2\% \mid \frac{7}{2};-\frac{3}{2}>$	0.001	0.001	3.380
	$98\% \mid \frac{7}{2};-\frac{3}{2}> + 2\% \mid \frac{7}{2};+\frac{3}{2}>$			
KD4	$88\% \mid \frac{7}{2};+\frac{1}{2}> + 12\% \mid \frac{7}{2};-\frac{1}{2}>$	4.563	4.562	1.132
	$88\% \mid \frac{7}{2};-\frac{1}{2}> + 12\% \mid \frac{7}{2};+\frac{1}{2}>$			
	[TmCp$_3$]$^-$			
KD1	$96\% \mid \frac{7}{2};+\frac{7}{2}> + 4\%\mid \frac{7}{2};-\frac{5}{2}>$	1.144	1.149	7.499
	$96\% \mid \frac{7}{2};-\frac{7}{2}> + 4\%\mid \frac{7}{2};+\frac{5}{2}>$			
KD2	$95\% \mid \frac{7}{2};+\frac{5}{2}> + 5\%\mid \frac{7}{2};-\frac{7}{2}>$	0.934	1.283	5.187
	$95\% \mid \frac{7}{2};-\frac{5}{2}> + 5\%\mid \frac{7}{2};+\frac{7}{2}>$			
KD3	$50\% \mid \frac{7}{2};-\frac{1}{2}> + 30\%\mid \frac{7}{2};-\frac{3}{2}> + 20\%\mid \frac{7}{2};+\frac{1}{2}>$	4.853	4.163	1.197
	$50\% \mid \frac{7}{2};+\frac{1}{2}> + 30\%\mid \frac{7}{2};+\frac{3}{2}> + 20\%\mid \frac{7}{2};-\frac{1}{2}>$			
KD4	$55\% \mid \frac{7}{2};+\frac{3}{2}> + 30\%\mid \frac{7}{2};+\frac{1}{2}> + 15\%\mid \frac{7}{2};-\frac{3}{2}>$	0.096	0.148	5.367
	$55\% \mid \frac{7}{2};-\frac{3}{2}> + 30\%\mid \frac{7}{2};-\frac{1}{2}> + 15\%\mid \frac{7}{2};+\frac{3}{2}>$			

Crystal Field analysis

The crystal field Hamiltonian fo4 a f complex in a pseudoaxial symmetry (D_{9h} or D_{9d}) and trigonal (D_{3h}) have, respectively, the form:

$$\hat{H}^{CF}(D_\infty) = B_2^0\hat{C}_2^0 + B_4^0\hat{C}_4^0 + B_6^0\hat{C}_6^0$$

$$\hat{H}^{CF}(D_{3h}) = B_2^0\hat{C}_2^0 + B_4^0\hat{C}_4^0 + B_6^0\hat{C}_6^0 + B_6^6\left(\hat{C}_6^{-6} + \hat{C}_6^6\right)$$

where B_k^q are the crystal field parameters and C_k^q are the spherical tensor operators. The matrix elements $< Jm_J \mid \hat{H}^{CF} \mid Jm_{J'} >$ are evauated by application of the operator equivalent techniques, where the spherical

tensor can be written a a functions of the total angular momentum operator and Stevens coefficients. Both Hamiltoians above can be rewritten as:

$$\hat{H}^{CF}(D_{\infty}) = \alpha_J B_2^0 \hat{O}_2^0 + \beta_J B_4^0 \hat{O}_4^0 + \gamma_J B_6^0 \hat{O}_6^0$$

$$\hat{H}^{CF}(D_{3h}) = \alpha_J B_2^0 \hat{O}_2^0 + \beta_J B_4^0 \hat{O}_4^0 + \gamma_J \left[B_6^0 \hat{O}_6^0 + B_6^6 \left(\hat{O}_6^{-6} + \hat{O}_6^6 \right) \right]$$

where α_J, β_J and γ_J are the Stevens coefficients. Particularly the equivalent operator $\hat{O}_k^q$ for k = 2, 4 have the form:

$$\hat{O}_2^0 = 3J_z^2 - J\left(J+1\right)$$

$$\hat{O}_4^0 = 35J_z^4 - 30J\left(J+1\right)J_z^2 + 25J_z^2 - 6J\left(J+1\right) + 3J^2\left(J+1\right)^2$$

In the case of Tm^{2+} ion the product $\alpha_J B_2^0 < 0$ requiere, to get estabililization, that $\hat{O}_2^0 > 0$. This is translated, by the form of the operator, in a ground state with a large value of m_J. On the other hand, when B_4^0 is also large, the introduction of cuadratic term favors intermediate values of m_J.

Table 7: Irreducible representations and equivalences between different point groups analyzed in this work

D_{9d}	D_{9h}	D_{3d}	D_{3h}	C_{3v}	Orbital
A_{2u}	A_2''	A_{2u}	A_2''	A_1	f_0
E_{1u}	E_1'	E_u	E'	E	$f_{\pm1}$
E_{2u}	E_2''	E_u	E''	E	$f_{\pm2}$
E_{3u}	E_3'	$A_{1u}\oplus A_{2u}$	$A_1'\oplus A_2'$	$A_1\oplus A_2$	$f_{\pm3}$
A_{1g}	A_1'	A_{1g}	A_1'	A_1	d_0
E_{1g}	E_1''	E_g	E''	E	$d_{\pm1}$
E_{2g}	E_2'	E_g	E'	E	$d_{\pm2}$